

**NASA TECHNICAL
MEMORANDUM**



NASA TM X-3218

NASA TM X-3218

**LOW-SPEED UPWASH INTERFERENCE ON
A TRANSPORT MODEL IN A RECTANGULAR
SLOTTED-WALL WIND TUNNEL**

Michael J. Mann

*Langley Research Center
Hampton, Va. 23665*



1. Report No. NASA TM X-3218		2. Government Accession No.		3. Recipient's Catalog No.	
4. Title and Subtitle LOW-SPEED UPWASH INTERFERENCE ON A TRANSPORT MODEL IN A RECTANGULAR SLOTTED-WALL WIND TUNNEL				5. Report Date August 1975	
				6. Performing Organization Code	
7. Author(s) Michael J. Mann				8. Performing Organization Report No. L-10042	
9. Performing Organization Name and Address NASA Langley Research Center Hampton, Va. 23665				10. Work Unit No. 505-06-42-03	
				11. Contract or Grant No.	
12. Sponsoring Agency Name and Address National Aeronautics and Space Administration Washington, D.C. 20546				13. Type of Report and Period Covered Technical Memorandum	
				14. Sponsoring Agency Code	
15. Supplementary Notes					
16. Abstract <p>A study has been made of the upwash interference caused by the wind-tunnel walls at a Mach number of 0.20. The wind tunnel has slotted horizontal walls and solid vertical walls and the wind-tunnel model is a wing-fuselage combination typical of a short take-off and landing (STOL) transport. Measurements were made of the model forces and angle of attack. The experimental results are compared to theoretical solutions for the upwash interference. This comparison enabled an indirect determination of one of the constants in the slotted-wall boundary condition. The magnitude of the experimental upwash interference is also compared to the accuracy of the data. This comparison indicates that it is difficult to make definite conclusions based on the experimental data. Suggestions are made for future research which could provide a practical means of accurately determining the wall-interference velocities in wind tunnels with rigid slotted walls.</p>					
17. Key Words (Suggested by Author(s)) Wall interference Wind-tunnel wall interference Upwash interference Lift interference				18. Distribution Statement Unclassified - Unlimited New Subject Category 02	
19. Security Classif. (of this report) Unclassified	20. Security Classif. (of this page) Unclassified	21. No. of Pages 25	22. Price* \$3.25		

LOW-SPEED UPWASH INTERFERENCE ON A TRANSPORT MODEL IN A RECTANGULAR SLOTTED-WALL WIND TUNNEL

Michael J. Mann
Langley Research Center

SUMMARY

A study has been made of the upwash interference caused by the wind-tunnel walls at a Mach number of 0.20. The wind tunnel has slotted horizontal walls and solid vertical walls and the wind-tunnel model is a wing-fuselage combination typical of a short take-off and landing (STOL) transport. Measurements were made of the model forces and angle of attack. The experimental results are compared to theoretical solutions for the upwash interference. This comparison enabled an indirect determination of one of the constants in the slotted-wall boundary condition. The magnitude of the experimental upwash interference is also compared to the accuracy of the data. This comparison indicates that it is difficult to make definite conclusions based on the experimental data. Suggestions are made for future research which could provide a practical means of accurately determining the wall-interference velocities in wind tunnels with rigid slotted walls.

INTRODUCTION

Wind-tunnel testing generally requires a large model in order to maximize the Reynolds number and to increase the accuracy of the model dimensions. Evaluation of airplane performance requires that wind-tunnel data be obtained with a high degree of accuracy. These dual requirements, a large model and accurate data, are conflicting because a large model is influenced by large wall-induced flow distortions. Accurate data require that the effects of these flow distortions be eliminated in order to simulate unconfined flight conditions. However, methods of eliminating wall-induced flow distortions are not yet well understood, especially in the case of ventilated walls. (See refs. 1 (p. 21), 2, and 3 (pp. 24-26).)

Elimination of the effects of these flow distortions or "wall-induced interference velocities" from the wind-tunnel data can be accomplished by two methods. One method, currently under development, is to alter the shape of the wind-tunnel walls during each experiment so that interference-free conditions exist. This approach is especially attractive for cases in which the flow is nonlinear, such as the transonic regime and

low-speed vertical and short take-off and landing (V/STOL) flight. (See ref. 4.) Low-speed V/STOL flight generally exhibits nonlinear effects when the wake undergoes large flow deflections.

The second method, which is in general use today, requires that the wind-tunnel data be "corrected" for the wall interference. This correction requires a knowledge of both the wall-induced interference velocities and the effects of these velocity perturbations on the aerodynamic data. In order to calculate the interference velocities, the wind-tunnel wall boundary condition must be known. Ventilated-wall test sections have been the subject of extensive theoretical study. It is generally recognized that an insufficient number of experimental wall-interference investigations have been made under actual wind-tunnel operating conditions in order to establish the wall boundary condition.

Once the interference velocities are computed, the problem still remains of determining their effects on the model. This problem is complicated, for example, by the variation of the induced upwash in the direction of the tunnel axis and across the wing span.

This study has been made in order to gain a better understanding of the slotted-wall boundary condition at subsonic speeds in a rectangular wind tunnel. A secondary objective was to gain an improved understanding of the wall-induced upwash-interference corrections which must be applied to the low-speed data obtained in the Langley high-speed 7- by 10-foot tunnel. Since the tunnel was restricted to low speed pending replacement of the fan blades, the study was conducted at a Mach number of 0.2. The method of replacing the exact slotted-wall boundary condition by an equivalent homogeneous boundary condition is discussed. The basic theoretical results are presented along with a discussion of the experimental methods used in determining the parameters in the boundary condition. A comparison has been made of the experimental and theoretical upwash interference for each of two slotted-wall configurations. The model consisted of a fuselage with an uncambered and untwisted swept wing. Difficulties in the experimental determination of the upwash interference are discussed and suggestions are made for future research.

SYMBOLS

Measurements and calculations were made in the U.S. Customary Units. They are presented herein in the International System of Units (SI) with the equivalent values given in the U.S. Customary Units.

a slot width, m (ft)

C wind-tunnel cross-sectional area, m^2 (ft^2)

C_L	model lift coefficient, $\frac{\text{Model lift}}{q_\infty S}$
C_p	pressure coefficient, $\frac{p - p_\infty}{q_\infty}$
d	distance between slot centers, m (ft)
h	semiheight of wind tunnel, m (ft)
K	geometric-slot parameter, m (ft) (eqs. (2) and (3))
M_∞	free-stream Mach number
n	coordinate in the direction of the outward normal of the wall, m (ft)
P	slot parameter, $\frac{1}{1 + (K/h)}$ (eq. (9))
p	local static pressure, N/m^2 (lbf/ft ²)
p_∞	free-stream static pressure, N/m^2 (lbf/ft ²)
q_∞	free-stream dynamic pressure, N/m^2 (lbf/ft ²)
R	porosity parameter, dimensionless
S	wing area, m ² (ft ²)
u	perturbation velocity in x-direction, m/sec (ft/sec)
V_∞	free-stream velocity, m/sec (ft/sec)
v_n	perturbation velocity in n-direction, m/sec (ft/sec)
w	upwash velocity, m/sec (ft/sec)
x	coordinate in direction of free stream, m (ft)
α	angle of attack measured between horizontal reference (determined by an inclinometer) and fuselage reference line (see ref. 14) and corrected for wind-tunnel flow angularity; positive direction is nose up, deg

$$\beta = \sqrt{1 - M_{\infty}^2}$$

Δ denotes a change in quantity which follows

δ upwash-interference factor (eq. (7))

ϕ perturbation-velocity potential, m^2/sec (ft^2/sec)

Subscript:

cor corrected for upwash interference

THEORETICAL BACKGROUND

The exact inviscid boundary conditions for a wall with slots parallel to the flow are

$$\frac{\partial \phi}{\partial n} = 0$$

at the slats, and

$$\frac{\partial \phi}{\partial x} = 0 \rightarrow \phi = 0$$

at the slots, where ϕ is the perturbation potential, x is the streamwise coordinate, and n is the coordinate in the direction of the outward normal to the wall. (See refs. 5, 6, and 7.) The actual slotted walls can be replaced by homogeneous walls which have the effect of the slots uniformly distributed over their surface. The effect at the model location of the homogeneous wall is assumed to approximate closely the effect of the actual wall. By assuming the slot flow to be inviscid, the boundary condition of the homogeneous wall (ref. 5) is

$$\frac{\partial \phi}{\partial x} + K \frac{\partial^2 \phi}{\partial x \partial n} = 0 \quad (1)$$

where K depends on the slot width and the number of slots. For a given wing span and tunnel cross section, the homogeneous wall concept permits calculation of the wall interference in terms of the single parameter K . However, the exact boundary conditions require a separate calculation for each combination of slot width and number of slots. (See refs. 7 and 8.)

The geometric-slot parameter K is theoretically defined in terms of the slotted-wall geometry. Davis and Moore (ref. 5) derive the following expression for K

$$K = \frac{d}{\pi} \ln \left(\csc \frac{\pi}{2} \frac{a}{d} \right) \quad (2)$$

where the wall is assumed to have zero thickness. Chen and Mears (ref. 6) derive an alternate expression for K which accounts for wall thickness. For a wall of zero thickness, their result is

$$K = \frac{d - a}{2} \tan \left[\frac{\pi}{2} \left(1 - \frac{a}{d} \right) \right] \quad (3)$$

In both equations (2) and (3), d is the distance between slot centers and a is the slot width. Since equations (1), (2), and (3) are based on a two-dimensional cross-flow model, the slots are assumed to be infinitely long. It is also assumed that the flow in adjacent slots is the same; therefore, the results apply to tunnels with several slots. The predictions of equations (2) and (3) are examined in the "Results and Discussion" section in order to determine how well each correlates with experimental data.

When the analysis leading to equation (1) is generalized to include the effects of the shearing stresses in the slot flow, the homogeneous boundary condition becomes

$$\frac{\partial \phi}{\partial x} + K \frac{\partial^2 \phi}{\partial x \partial n} + \frac{\beta}{R} \frac{\partial \phi}{\partial n} = 0 \quad (4)$$

where the porosity parameter R is an empirical constant intended to account for viscous effects. (See refs. 9 and 10.) The parameter $\beta = \sqrt{1 - M_\infty^2}$ accounts for compressibility.

Holder (ref. 10) has calculated the upwash interference in a rectangular wind tunnel using equation (4) as a boundary condition. Holder's results show that viscosity reduces the effective slot width so that the interference is shifted in the direction of the closed wall interference. His results are used in the "Results and Discussion" section of this paper in order to examine the experimental results.

Keller (ref. 11) has developed a numerical method of calculating wall interference which utilizes equation (4). Keller's method permits finite-length slots with varying width. Since the model can be located anywhere in the test section, this method also permits movement of the model off the wind-tunnel center line.

Writing equation (4) in terms of the velocity components gives

$$\frac{u}{V_\infty} + K \frac{\partial}{\partial x} \frac{v_n}{V_\infty} + \frac{\beta}{R} \frac{v_n}{V_\infty} = 0 \quad (5)$$

The quantity v_n/V_∞ is the flow angle and the u/V_∞ term is related to the pressure difference across the wall. Assuming that the pressure outside the wall (plenum pressure) equals the free-stream static pressure, small-perturbation theory yields the result

$$C_p = -2 \frac{u}{V_\infty} \quad (6)$$

where C_p is the pressure coefficient at a point inside the tunnel at the wall. (See ref. 5.) The term in equation (5) $K \frac{\partial}{\partial x} \frac{v_n}{V_\infty}$ represents the momentum flux across the equivalent homogeneous wall. (See refs. 5 and 12 (p. 48).)

Binion (ref. 13) has made an experimental study of the slotted-wall boundary condition for a wind tunnel with slotted horizontal and solid vertical walls. Indirect measurements, that is, measurements which were made at the model rather than at the wall itself, were used for studying the wall boundary condition. The measurements made at the model were measurements of forces and angle of attack. In order to obtain interference-free data, measurements were also made in a wind tunnel whose dimensions were large when compared to the model. By use of equation (1) as the slotted-wall boundary condition, it was found that equation (3) correlated better with the experimental results than equation (2).

In the present study, the viscous term of the slotted-wall boundary condition has been indirectly determined. Measurements were made of the forces and angle of attack of a model mounted in both closed and slotted test sections. The closed-wall data were corrected for wall interference and regarded as interference free. These interference-free data were then used to determine experimental upwash-interference corrections for the slotted test sections.

Alternately, it is possible to determine directly the slotted-wall boundary condition by measurement of the pressure and flow angle inside the tunnel in the vicinity of the wall. By use of equations (5) and (6), these measurements would permit determination of K and R .

EXPERIMENTAL EQUIPMENT AND TEST CONDITIONS

The wind-tunnel model was a wing-fuselage combination typical of a STOL transport. (See fig. 1.) The model had a high wing with a quarter-chord sweep of 20° and zero twist. The wing area was 0.483 m^2 (5.202 ft^2) and the wing span was 1.902 m (6.24 ft). The airfoil section varied from an NACA 65A 015 at the wing root to an NACA 65A 010 at the wing tip. Transition strips of carborundum grit number 60 were 0.15 cm (0.06 in.) wide and were placed 2.54 cm (1 in.) aft of the wing and fuselage leading edges. The maximum fuselage diameter was 23.9 cm (9.4 in.) and the fuselage length was 207.26 cm (81.60 in.). The same model, with an empennage added, is configuration 0 of reference 14, which may be consulted for additional details.

The tests were conducted in the Langley high-speed 7- by 10-foot tunnel. This is a continuous-flow, atmospheric wind tunnel with solid vertical walls and slotted horizontal walls. The test-section dimensions are 292.1 cm (115 in.) wide by 200.7 cm (79 in.)

high. The horizontal walls were run closed and slotted at 6.4- and 18.8-percent open ratio.¹ The slot spacing was equal to one-fourth of the test-section width. The wind-tunnel slot arrangement and model location are shown in figure 1.

The model was mounted on a sting attached to a vertical strut. The angle-of-attack mechanism produced an approximate rotation of the model about a point located 45.5 cm (17.9 in.) aft of the quarter-chord point of the wing mean aerodynamic chord. Thus, the displacement of the wing from the tunnel center line with changes in angle of attack was restricted to small values. This experimental arrangement more nearly duplicated the theoretical models investigated in this study, since these models assume the lifting surface to be on the tunnel center line.

The average flow conditions in the test section resulted in a total temperature of 9.9° C (49.9° F) and a dynamic pressure of 2789.0 N/m² (58.25 lbf/ft²). These conditions gave a Reynolds number of $4.66 \times 10^6/\text{m}$ ($1.42 \times 10^6/\text{ft}$) and a Mach number of 0.20.

The data were corrected for flow angularity. The model was tested both upright and inverted for each horizontal wall configuration. The flow angularity was determined by a comparison of the lift curves (C_L plotted against α) for the upright and inverted positions. For the horizontal walls closed and slotted at 6.4- and 18.8-percent open ratio, the magnitudes of the flow angle corrections were 0.03°, 0.065°, and 0°, respectively.

Herriot's method (ref. 15) was used to make a blockage correction to the data obtained with the closed-wall configuration; over the lift-coefficient range, $|\Delta q_\infty|/q_\infty$ varied² from 0.0099 to 0.0107. The solid blockage of the slotted-wall configurations was estimated by using the boundary condition of equation (1) and by assuming K to lie between the values given by equations (2) and (3). For this range of values of K , reference 16 showed that the solid blockage interference of the slotted-wall configurations can be neglected.

Model forces were measured with a six-component strain-gage balance. Measurements were made of the balance chamber pressure in order to correct the axial-force data to a condition of free-stream static pressure acting on the fuselage base. The angle of attack was measured by two pendulous, inertial, single-axis accelerometers (closed-loop type). Since the accelerometers had differences in their method of damping, material of construction, and electronics, their results provided a means of corroboration.

Table I summarizes the accuracy of the instrumentation used in measuring lift and angle of attack. The balance accuracy was obtained by static multicomponent load tests

¹ Percent open ratio is the total percent of the horizontal walls which are open. Since each horizontal wall has four slots spaced at one-fourth of the tunnel width, percent open ratio equals 100 (a/d).

² An estimate of the change in C_L caused by a change in q_∞ can be obtained from $|\Delta C_L| = (|\Delta q_\infty|/q_\infty) C_L$.

on the balance. The accelerometer plus data-acquisition system accuracy was determined by making four angle-of-attack calibrations using an inclinometer. Two calibrations were made with the model in the upright position and two in the inverted position; both accelerometers were calibrated on each calibration. By assuming the same output signal from the data-acquisition system, the maximum spread in the indicated angle of attack for a given accelerometer was taken as the accuracy of that accelerometer. The accuracy of the inclinometer was determined by the use of a precision level and a dividing head.

RESULTS AND DISCUSSION

Results for accelerometer A are shown in figures 2 to 4. Figure 2 shows the lift curves for each wall configuration without an upwash-interference correction.

Figure 3 shows the lift curves for each configuration where only the closed-wall data have been corrected for upwash interference. The method of reference 17 was used to determine the closed-wall correction. This method assumes an elliptic-spanwise load distribution and includes the effects of streamline curvature and corrections to lifting-line theory obtained from lifting-surface theory. The closed-wall correction of reference 17 was the same within the accuracy of the angle-of-attack data as the corrections of references 18, 19, and 20, which have slightly different assumptions. Calculations based on the method of reference 20 indicated that the spanwise variation of the upwash interference (between the 10- and 90-percent semispan stations) was about 27 percent of the average value of the upwash interference. All the theoretical values of the upwash-interference corrections (closed and slotted walls) presented in this study are mean values obtained by integrating the interference across the wing span.

Since the closed-wall boundary condition is known, the corrected closed-wall data are assumed to be interference free. Therefore, an experimental upwash-interference correction for both of the slotted-wall experiments can be determined from figure 3. The upwash-interference factor δ is defined as

$$\delta \equiv \frac{\Delta\alpha}{C_L} \frac{C}{S} \frac{\pi}{180} \quad (7)$$

where C is the wind-tunnel cross-sectional area and S is the wing area. The quantity $\Delta\alpha$ (in degrees) is given by

$$\Delta\alpha = \frac{w}{V_\infty} \frac{180}{\pi}$$

where w is the upwash velocity and V_∞ is the free-stream velocity. For a given value of C_L , the $\Delta\alpha$ is the increment in the angle of attack between the slotted-wall

data and the interference-free data. Hence, $\Delta\alpha$ becomes the experimental upwash-interference correction to the lift curve.

From figure 3, it can be seen that in the case of the 6.4-percent open ratio the value of $\Delta\alpha/C_L$ (and therefore of δ) is a function of angle of attack. Since the slope of the lift curve decreases³ at the higher angles of attack, and a loss of accuracy in $\Delta\alpha$ occurs at the lower angles of attack, the $\Delta\alpha/C_L$ was determined at several points between a C_L of 0.22 and 0.34. These values of $\Delta\alpha/C_L$ were averaged, and the corrected angle of attack was computed by

$$\alpha_{\text{cor}} = \alpha + \frac{\Delta\alpha}{C_L} C_L \quad (8)$$

where α is the measured angle of attack shown in figure 3.

The results of this procedure are shown in figure 4 where the corrected slotted-wall data are compared to the interference-free data. It is seen that the single $\Delta\alpha/C_L$ determined for each slotted wall brings the data for that wall into relatively good agreement with the interference-free data over the angle-of-attack range.

Since the transformation from the measured normal- and axial-force components to the lift- and drag-force components requires a knowledge of α , the angle correction of equation (8) causes a slight change in C_L . However, this change in C_L is within the accuracy of the balance and has therefore been ignored.

Figures 5 to 7 present the corresponding results for accelerometer B. Since several calibrations were made for both accelerometers and differing types of accelerometers were used, the results for accelerometers A and B provide a means of corroboration.

Figures 8 and 9 show a comparison between the theoretical and experimental upwash-interference factors, and also provide a direct comparison of the results of accelerometers A and B. The slot parameter P is defined by

$$P = \frac{1}{1 + \frac{K}{h}} \quad (9)$$

where h is the wind-tunnel semiheight. A closed wall corresponds to $P = 0$, and a completely open horizontal wall corresponds to $P = 1$ (and $R/\beta = \infty$). The theoretical curves are the same in both figures, but the experimental results differ because of different methods of computing K from the wind-tunnel geometry.

³ Since the wing had zero twist, the decrease in slope of the lift curve may have been caused by wing-tip stall. In addition, the spanwise variation in $\Delta\alpha$ was calculated for the closed-wall case and was found to have been a possible factor in promoting wing-tip stall at the higher lift coefficients.

The theoretical results were obtained by Holder (ref. 10) using equation (4) for the slotted-wall boundary condition. Holder's results have been extrapolated to the present ratio of wing span to tunnel width. A lifting line with a uniform-load distribution has been used to represent the model. The upwash-interference factor δ has been integrated across the span to obtain an average value. Kraft (ref. 18) has made calculations for $R/\beta = \infty$ (inviscid flow) which are in good agreement with the corresponding results shown in figures 8 and 9.

Since the porosity parameter R is a constant which must be determined experimentally, theoretical results using equation (4) are semiempirical. As shown in figures 8 and 9, the viscous effects are assumed to vary from zero ($R/\beta = \infty$) to a magnitude which prevents any flow through the slot ($R/\beta = 0$).

The experimental values of δ in figures 8 and 9 were determined from figures 3 and 6 as previously discussed. In terms of angle of attack, the results for the two accelerometers agree within 0.06° at the highest lift coefficient. In order to calculate the value of P for the experimental results, a method of relating K to the experimental arrangement must be chosen. Figure 8 shows the results when the method of Davis and Moore is used. (See eq. (2).) Figure 9 shows the results when the method of Chen and Mears is used. (See eq. (3).)

From figures 8 and 9 it is seen that only the method of Davis and Moore permits a correlation between the theory and the experiment for both slot conditions.⁴ Figure 8 indicates that the 6.4-percent open ratio (smaller value of P) has significant viscous effects; however, the 18.8-percent open ratio does not. This is a reasonable result, since it is expected that the effect of the boundary layer would be more pronounced in the more narrow slot. Figure 8 provides an indirect determination of R for each of the slotted-wall configurations. Therefore, the slotted-wall boundary condition can be completely defined by use of equations (2) and (4).

Comparison of the present results with unpublished data obtained previously on a smaller model at a Mach number of 0.6 in the Langley high-speed 7- by 10-foot tunnel indicates that the upwash interference (and therefore K and/or R) depends on the geometry of the model and/or the Mach number. The present results also show that R depends on slot width and apparently on the ratio of boundary-layer thickness to slot

⁴ Subsequent to the present analysis, Richard W. Barnwell of the Langley Research Center found that the surface streamline of the slat in the Chen and Mears theory produces a slot width which is smaller than the doublet rod spacing, whereas Chen and Mears assumed these distances to be equal. Calculations by Barnwell showed that for the 6.4- and 18.8-percent open ratios, P assumes values of 0.47 and 0.67, respectively (compared with 0.23 and 0.51 in fig. 9). This considerably reduces the disagreement indicated in figures 8 and 9 between the two theories, and in terms of δ in figure 10, the difference is reduced to a maximum of 0.04 for $R/\beta = \infty$ (which translates into 0.1° in α at $C_L = 0.6$).

width. The upwash interference was found to depend on angle of attack for the 6.4-percent open ratio. Furthermore, the survey article of Vayssaire (ref. 2) indicates that R depends on Mach number, angle of attack, model size, boundary-layer properties, slot geometry, and so forth. Hence, it would not seem that the results shown in figures 8 and 9 would apply to every test in the Langley high-speed 7- by 10-foot tunnel with the same wall configurations. Indeed, a great deal of experimental research needs to be carried out in order to define the effect of the foregoing parameters.

A difficulty exists in the interpretation of the results shown in figures 8 and 9. The magnitude of the experimental $\Delta\alpha$ ranged from 0.07° to 0.17° . Comparison of these values to the accuracy of the data as given in table I indicates that it is difficult to make definite conclusions with regard to the correct values of K and R .

Since the wall geometry is more easily visualized in terms of percent open ratio rather than slot parameter P , the results of figure 8 are presented in figure 10 in terms of percent open ratio.⁵ The dashed curve gives the best estimate of the variation of δ for this model at $M_\infty = 0.20$. This curve was faired through the data and coincides with the inviscid theory for open ratios greater than 18.8 percent; for open ratios less than 6.4 percent, the curve was faired through the closed wall solution. From this curve it is possible to estimate the value of R for any slot width.

CONCLUDING REMARKS

A study has been made of the upwash interference in two slotted wind-tunnel configurations. A homogeneous boundary condition containing the unknown constants K and R was used for calculating the upwash interference. It was found that by the use of the Davis and Moore method for calculating the geometric slot parameter K and by inclusion of the effects of viscosity in the slot flow with the porosity parameter R , it is possible to correlate the theoretical and experimental values of the upwash-interference factor δ . This correlation resulted in an indirect determination of R , since the measurements were made at the model rather than at the wall itself.

It has been noted that K and R apparently do not depend solely on the slotted-wall geometry. These parameters may also depend on model geometry, model angle of attack, Mach number, boundary-layer properties, and so forth.

A difficulty exists in the interpretation of the results of this study. The magnitude of the experimental $\Delta\alpha$ caused by upwash interference ranged from 0.07° to 0.17° .

⁵A method of relating K to the experimental arrangement must be selected for the theory in figure 10. In figures 8 and 9 it was necessary to make this selection for the experimental results.

Comparison of these values to the accuracy of the data indicated that it is difficult to make definite conclusions with regard to the correct values of K and R .

Experimental determination of the slotted-wall boundary condition by direct measurements would provide an independent check on the indirect measurements. Direct determination would involve measurement of the static pressure and flow angle inside the tunnel in the vicinity of the slotted wall. Combining these measurements with the slotted-wall boundary condition would permit determination of K and R . This method of approach is presently under study by several investigators.

With additional research, it may be established that the slotted-wall boundary condition depends on a variety of test conditions, varies substantially in the streamwise direction, and differs between the upper and the lower walls. In this case, an array of sensors near the slotted wall would be the only practical and accurate means of defining the wall boundary condition for each experiment. The interference-free, adjustable-wall wind-tunnel concept utilizes this direct method of evaluating wall interference. In the interference-free tunnel, the measurements are employed to alter the shape of the walls in order to eliminate the wall interference. In the fixed-wall tunnel, the measurements would be used for determining what wall-interference effects were present at each test point. A method such as Keller's numerical technique, which permits variation of the boundary condition along the walls, could be used for a more realistic calculation of the upwash interference.

Langley Research Center,
National Aeronautics and Space Administration,
Hampton, Va., April 16, 1975.

REFERENCES

1. Lukasiewicz, J., ed.: Aerodynamic Test Simulation: Lessons From the Past and Future Prospects. AGARD Rep. No. 603, Dec. 1972.
2. Vayssaire, Jean-Ch.: Survey of Methods for Correcting Wall Constraints in Transonic Wind Tunnels. Problems in Wind Tunnel Testing Techniques. AGARD Rep. No. 601, Apr. 1973.
3. Anon.: A Review of Current Research Aimed at the Design and Operation of Large Windtunnels. AGARD-AR-68, Mar. 1974.
4. Sears, W. R.: Self-Correcting Wind Tunnels. Rep. No. RK-5070-A-2 (Contract No. N00014-72-C-0102), Calspan Corp., July 1973. (Available from DDC as AD 764 957.)
5. Davis, Don D., Jr.; and Moore, Dewey: Analytical Study of Blockage- and Lift-Interference Corrections for Slotted Tunnels Obtained by the Substitution of an Equivalent Homogeneous Boundary for the Discrete Slots. NACA RM L53E07b, 1953.
6. Chen, C. F.; and Mears, J. W.: Experimental and Theoretical Study of Mean Boundary Conditions at Perforated and Longitudinally Slotted Wind Tunnel Walls. AEDC-TR-57-20, DDC Doc. No. AD 144 320, U.S. Air Force, Dec. 1957.
7. Wright, Ray H.; and Ward, Vernon G.: NACA Transonic Wind-Tunnel Test Sections. NACA Rep. 1231, 1955. (Supersedes NACA RM L8J06.)
8. Matthews, Clarence W.: Theoretical Study of the Tunnel-Boundary Lift Interference Due to Slotted Walls in the Presence of the Trailing-Vortex System of a Lifting Model. NACA Rep. 1221, 1955. (Supersedes NACA RM L53A26.)
9. Baldwin, Barrett S., Jr.; Turner, John B.; and Knechtel, Earl D.: Wall Interference in Wind Tunnels With Slotted and Porous Boundaries at Subsonic Speeds. NACA TN 3176, 1954.
10. Holder, D. R.: Upwash Interference on Wings of Finite Span in a Rectangular Wind Tunnel With Closed Side Walls and Porous-Slotted Floor and Roof. R. & M. No. 3395, British A.R.C., 1963.
11. Keller, James D.: Numerical Calculation of Boundary-Induced Interference in Slotted or Perforated Wind Tunnels Including Viscous Effects in Slots. NASA TN D-6871, 1972.
12. Kuethe, A. M.; and Schetzer, J. D.: Foundations of Aerodynamics. Second ed., John Wiley & Sons, Inc., c.1959.

13. Binion, Travis Weldon, Jr.: Wind Tunnel Wall Interference With a High Disc Loading V/STOL Model. M.S. Thesis, Univ. of Tennessee, 1971.
14. Thomas, James L.; Hoad, Danny R.; and Croom, Delwin R.: Aerodynamic Effects of Five Lift-Fan Pod Arrangements on an Unpowered V/STOL Transport Model. NASA TN D-7199, 1973.
15. Herriot, John G.: Blockage Corrections for Three-Dimensional-Flow Closed-Throat Wind Tunnels, With Consideration of the Effect of Compressibility. NACA Rep. 995, 1950. (Supersedes NACA RM A7B28.)
16. Rogers, E. W. E.: Wall Interference in Tunnels With Ventilated Walls. Subsonic Wind Tunnel Wall Corrections, H. C. Garner, ed., AGARDograph 109, Oct. 1966, pp. 341-429.
17. Garner, H. C.: Lift Interference on Three-Dimensional Wings. Subsonic Wind Tunnel Wall Corrections, H. C. Garner, ed., AGARDograph 109, Oct. 1966, pp. 75-217.
18. Kraft, E. M.: Upwash Interference on a Symmetrical Wing in a Rectangular Ventilated Wall Wind Tunnel: Part 1 - Development of Theory. AEDC-TR-72-187, U.S. Air Force, Mar. 1973.
19. Gillis, Clarence L.; Polhamus, Edward C.; and Gray, Joseph L., Jr.: Charts for Determining Jet-Boundary Corrections for Complete Models in 7- by 10-Foot Closed Rectangular Wind Tunnels. NACA WR L-123, 1945. (Formerly ARR L5G31.)
20. Heyson, Harry H.: Use of Superposition in Digital Computers To Obtain Wind-Tunnel Interference Factors for Arbitrary Configurations, With Particular Reference to V/STOL Models. NASA TR R-302, 1969.

TABLE I.- ACCURACY OF MEASURED VARIABLES

Measured variable	Instrument affecting measurement			
	Balance	Accelerometer plus data-acquisition system	Manometer	Inclinometer
C_L	0.001	^a 0.0000	0.004	0.0000
α , accelerometer A	----	.015 ^o	----	.01 ^o
α , accelerometer B	----	.03 ^o	----	.01 ^o

^a Effect of 0.03^o error in angle-of-attack measurement when transforming from normal and axial components of force to lift and drag components.

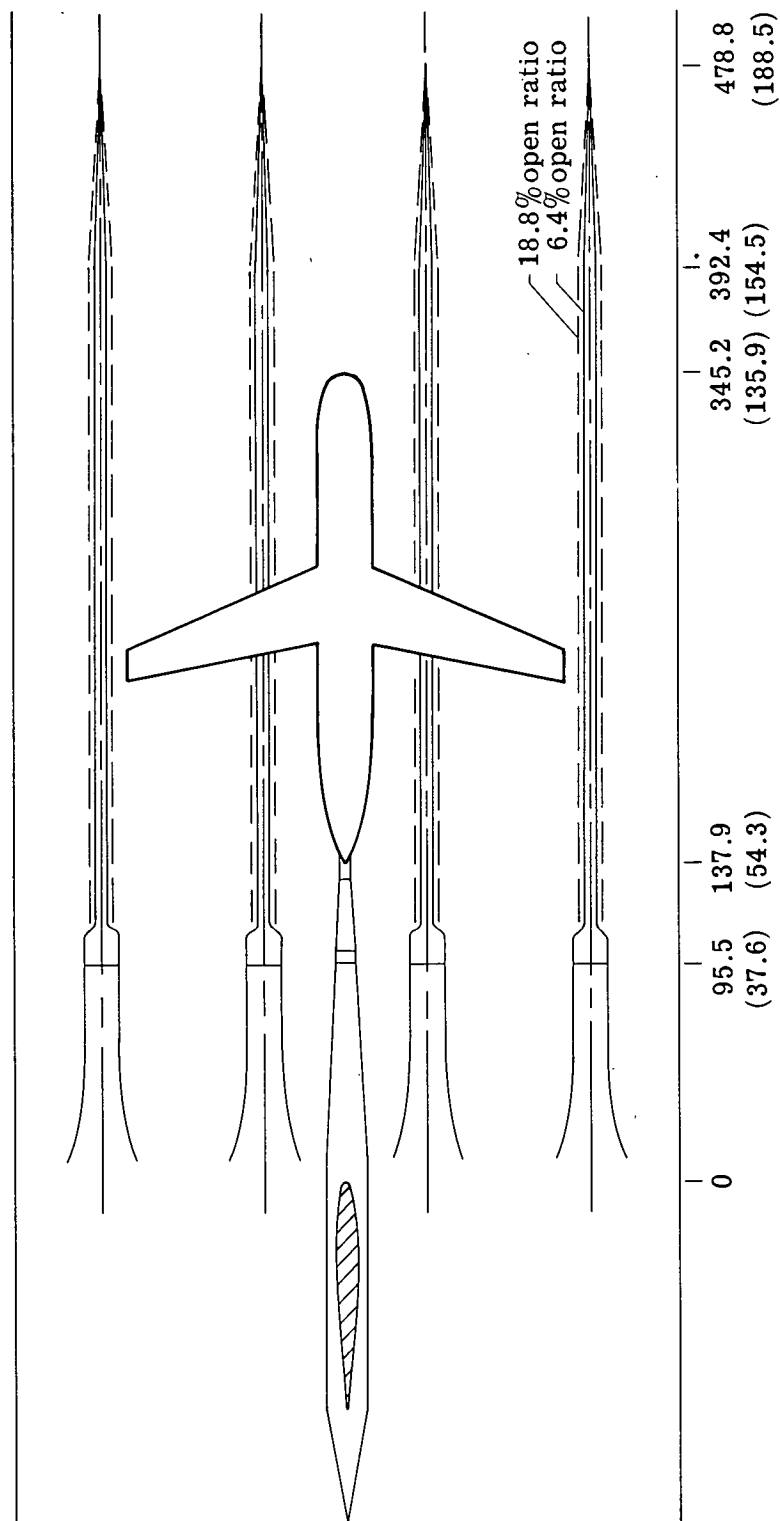


Figure 1.- Wind-tunnel arrangement. (Dimensions in cm (in.).)

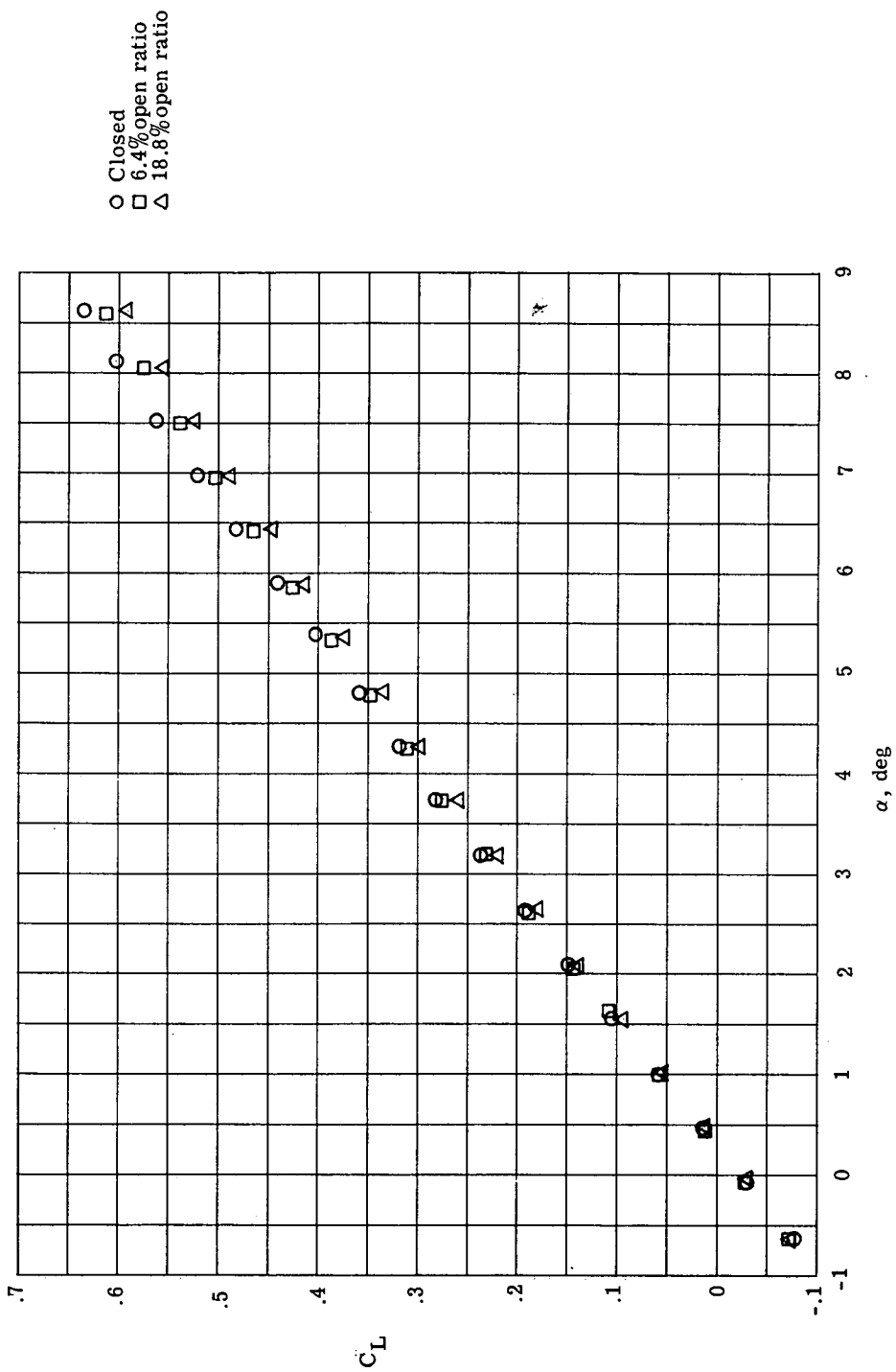


Figure 2.- Lift coefficient plotted against angle of attack without upwash-interference correction for three wall configurations. Accelerometer A.

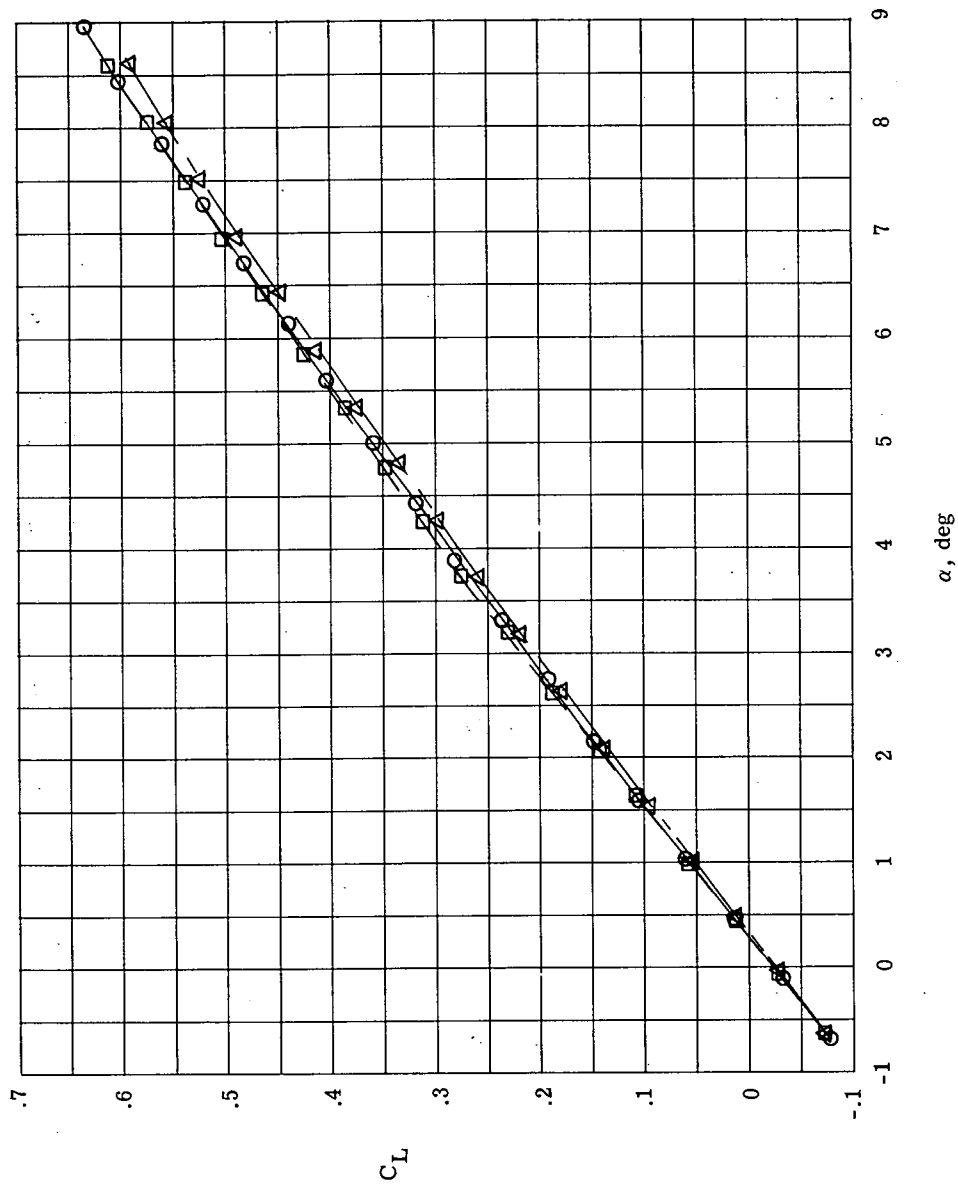


Figure 3.- Lift coefficient plotted against angle of attack for three wall configurations. Accelerometer A.

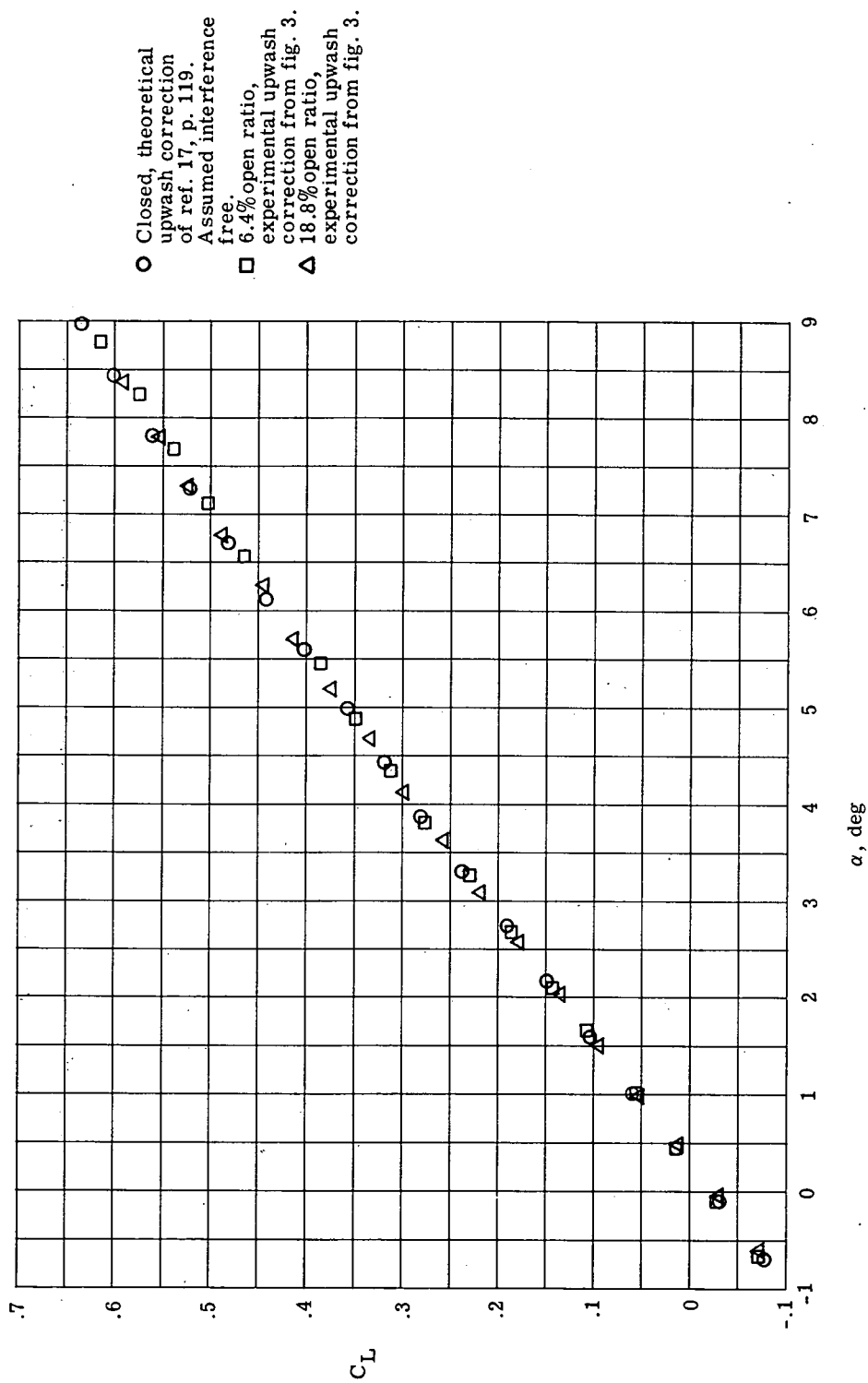


Figure 4.- Lift coefficient plotted against angle of attack with upwash-interference correction for three wall configurations. Accelerometer A.

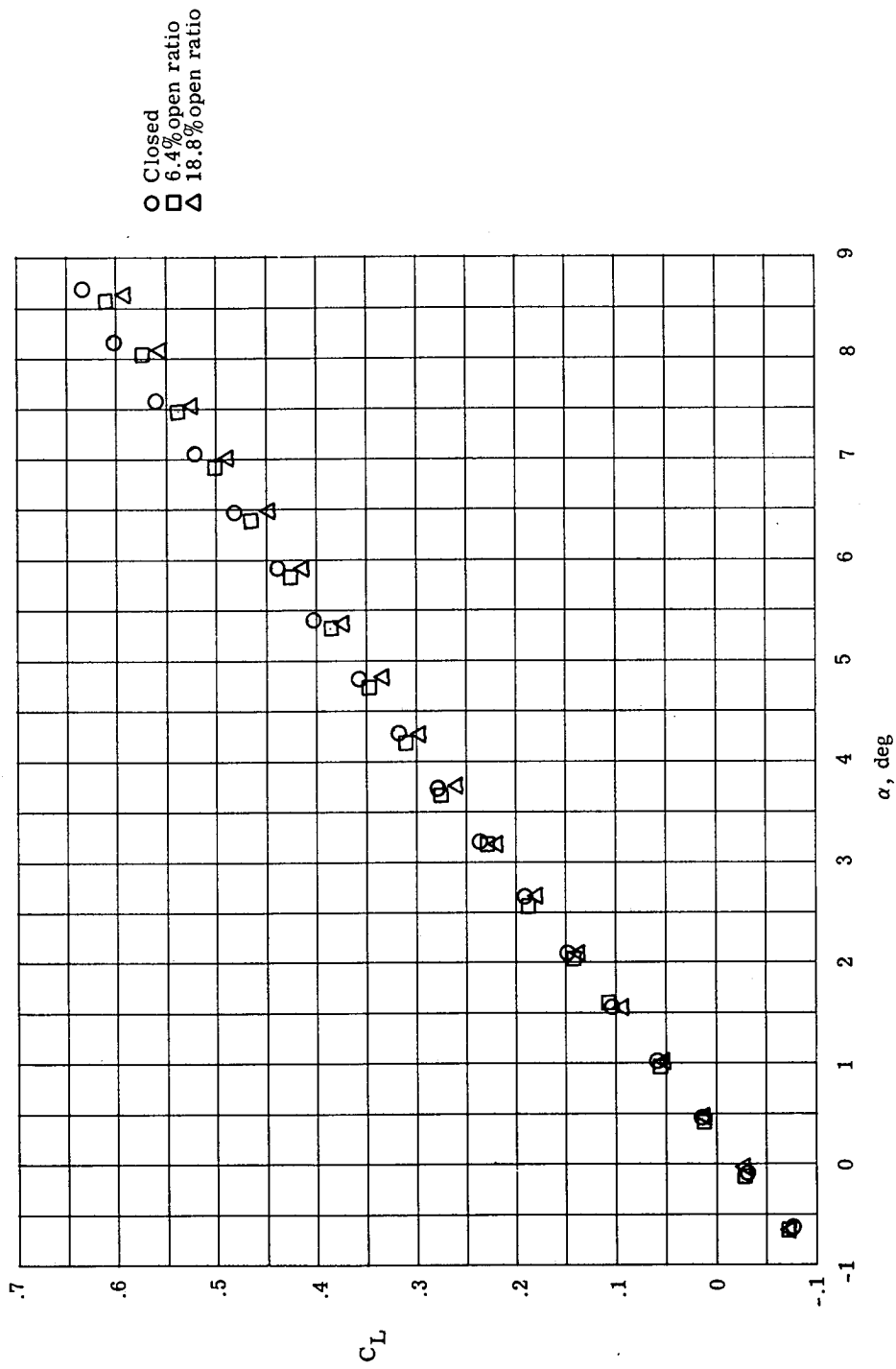


Figure 5.- Lift coefficient plotted against angle of attack without upwash-interference correction for three wall configurations. Accelerometer B.

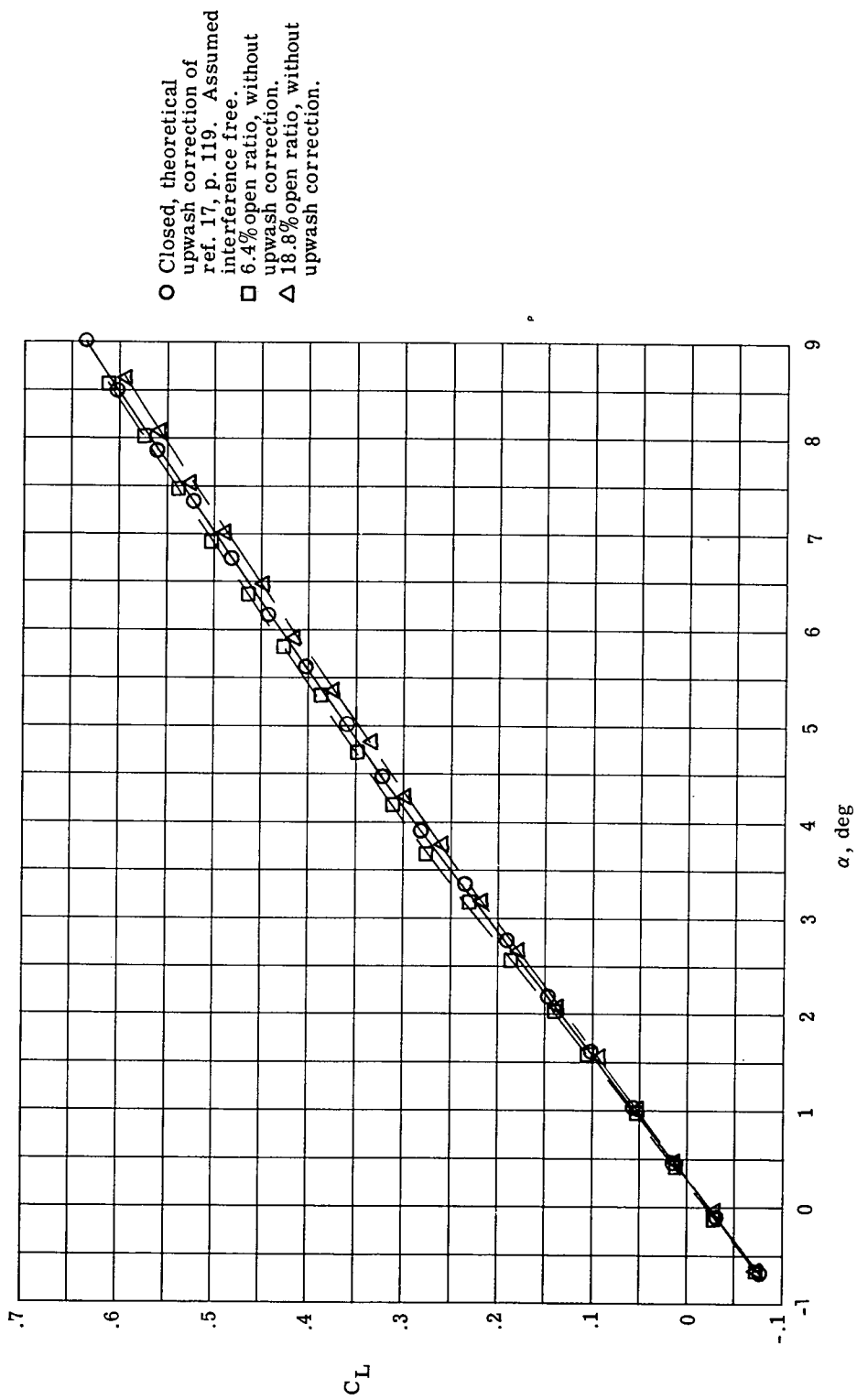


Figure 6.- Lift coefficient plotted against angle of attack for three wall configurations. Accelerometer B.

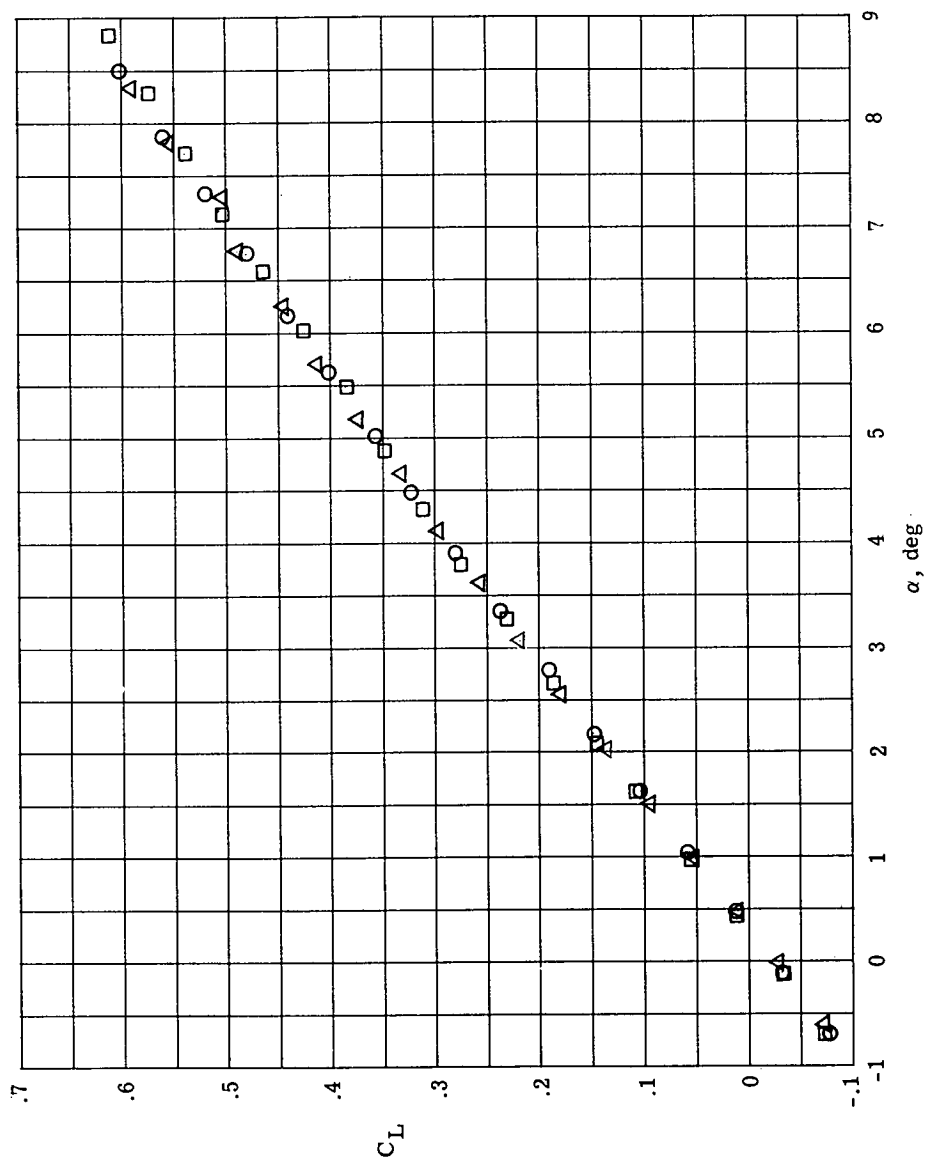


Figure 7.- Lift coefficient plotted against angle of attack with upwash-interference correction for three wall configurations. Accelerometer B.

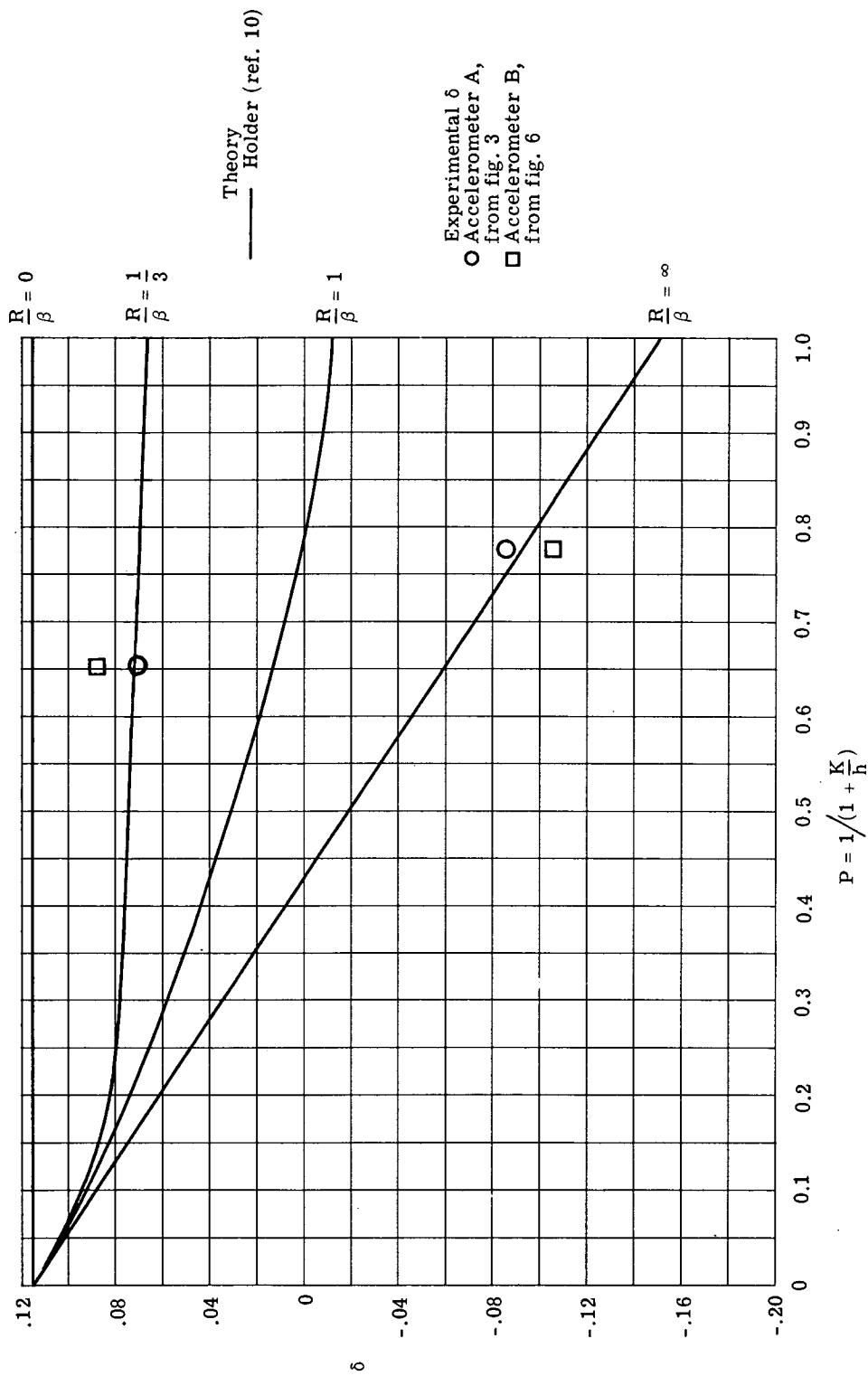


Figure 8.- Theoretical and experimental variation of upwash-interference factor δ with slot parameter P . Theoretical levels of slot-flow viscous effects indicated by R/β . Experimental value of P determined by calculating K from equation (2) (method of Davis and Moore, ref. 5).

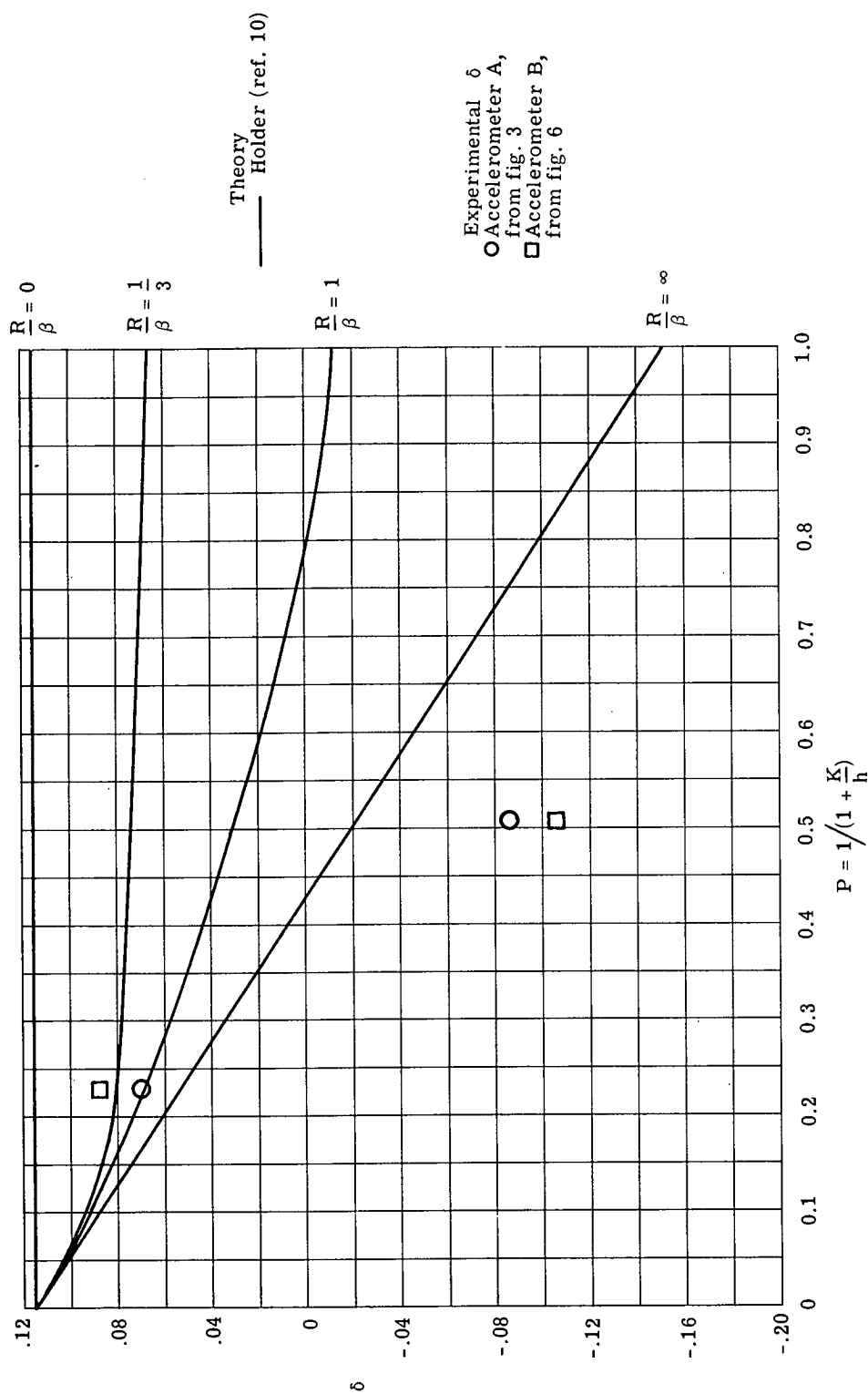


Figure 9.- Theoretical and experimental variation of upwash-interference factor δ with slot parameter P . Theoretical levels of slot-flow viscous effects indicated by R/β . Experimental value of P determined by calculating K from equation (3) (method of Chen and Mears, ref. 6).

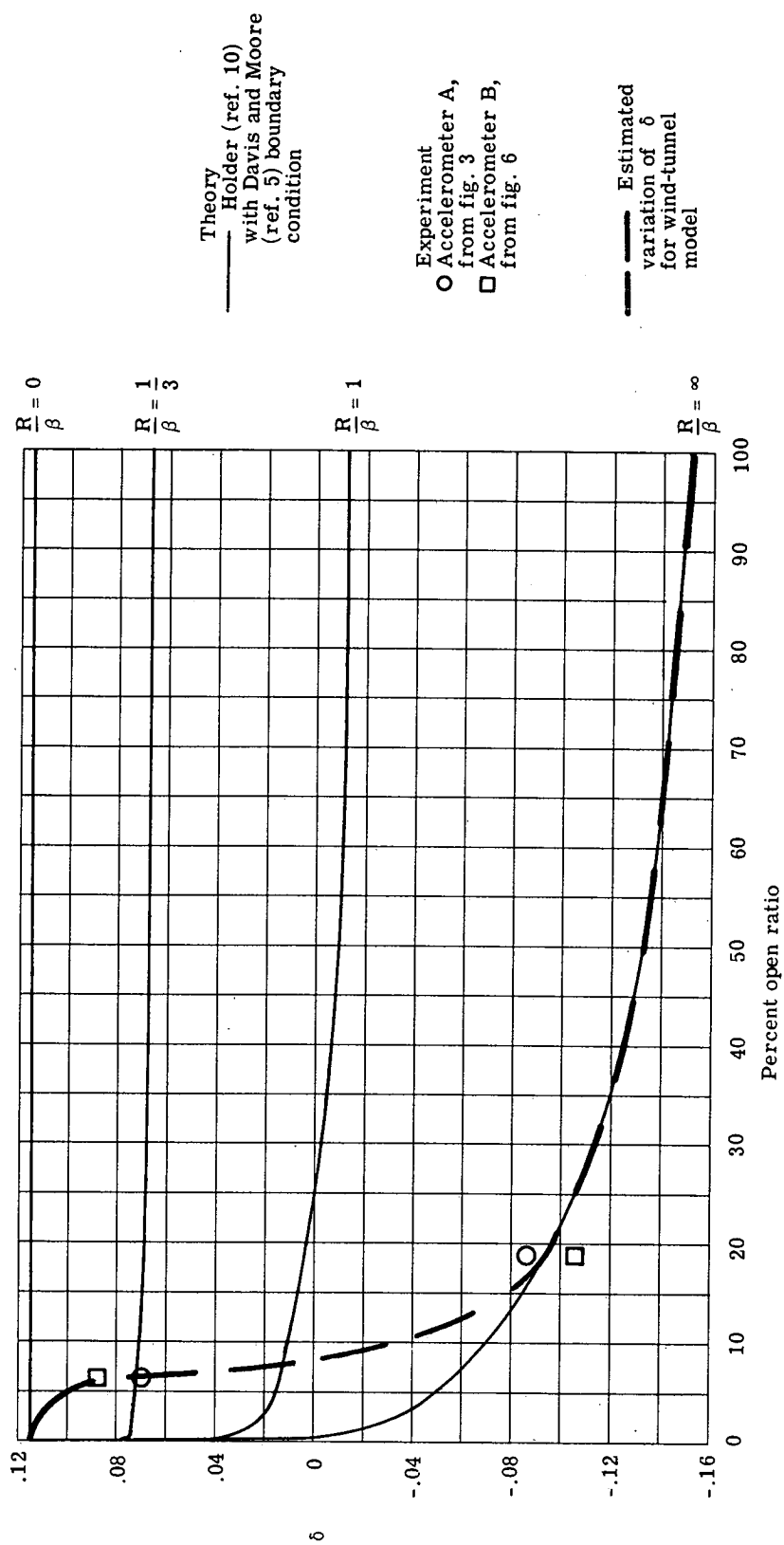


Figure 10.- Theoretical and experimental variation of upwash-interference factor δ with percent open ratio. Theoretical levels of slot-flow viscous effects indicated by R/β .



POSTMASTER : If Undeliverable (Section 158
Postal Manual) Do Not Return

"The aeronautical and space activities of the United States shall be conducted so as to contribute . . . to the expansion of human knowledge of phenomena in the atmosphere and space. The Administration shall provide for the widest practicable and appropriate dissemination of information concerning its activities and the results thereof."

—NATIONAL AERONAUTICS AND SPACE ACT OF 1958

NASA SCIENTIFIC AND TECHNICAL PUBLICATIONS

TECHNICAL REPORTS: Scientific and technical information considered important, complete, and a lasting contribution to existing knowledge.

TECHNICAL NOTES: Information less broad in scope but nevertheless of importance as a contribution to existing knowledge.

TECHNICAL MEMORANDUMS: Information receiving limited distribution because of preliminary data, security classification, or other reasons. Also includes conference proceedings with either limited or unlimited distribution.

CONTRACTOR REPORTS: Scientific and technical information generated under a NASA contract or grant and considered an important contribution to existing knowledge.

TECHNICAL TRANSLATIONS: Information published in a foreign language considered to merit NASA distribution in English.

SPECIAL PUBLICATIONS: Information derived from or of value to NASA activities. Publications include final reports of major projects, monographs, data compilations, handbooks, sourcebooks, and special bibliographies.

TECHNOLOGY UTILIZATION PUBLICATIONS: Information on technology used by NASA that may be of particular interest in commercial and other non-aerospace applications. Publications include Tech Briefs, Technology Utilization Reports and Technology Surveys.

Details on the availability of these publications may be obtained from:

SCIENTIFIC AND TECHNICAL INFORMATION OFFICE

NATIONAL AERONAUTICS AND SPACE ADMINISTRATION

Washington, D.C. 20546